International Journal for Parasitology 55 (2025) 461–474

Contents lists available at ScienceDirect

International Journal for Parasitology

journal homepage: www.elsevier.com/locate/ijpara

Dirofilaria asiatica sp. nov. (Spirurida: Onchocercidae) – Defined using a combined morphological-molecular approach

Vito Colella *, Neil D. Young, Ralph Manzanell, Ushani Atapattu, Sunita B. Sumanam, Lucas G. Huggins, Anson V. Koehler, Robin B. Gasser

Department of Veterinary Biosciences, Faculty of Science, The University of Melbourne, Parkville, VIC 3010, Australia

ARTICLE INFO

Article history:
Received 31 October 2024
Received in revised form 25 February 2025
Accepted 3 April 2025
Available online 8 April 2025

Keywords:
Zoonosis
Asia
Dogs
Dirofilariosis
Onchocercidae

ABSTRACT

Parasitic nematodes of the family Onchocercidae (superfamily Filarioidea) have evolved alongside vertebrate hosts for millions of years. While morphological methods have played a central role in identifying species, many taxa remain cryptic and are challenging to differentiate, complicating diagnosis and the understanding of their epidemiology. Among the clinically relevant genera are *Onchocerca* and *Dirofilaria*, the latter being responsible for illnesses such as heartworm disease in canines and rare zoonotic infections in humans. Despite advances in our knowledge of the canine heartworm (*Dirofilaria immitis*), substantial gaps remain regarding other *Dirofilaria* spp. and genotypes, and their impact on both animal and human health. In this study, we conducted the first known comprehensive morphological and molecular characterisation of a novel *Dirofilaria* sp., *Dirofilaria asiatica* sp. nov., from *Canis lupus familiaris* in Sri Lanka. This new species, genetically consistent with a previously identified novel genotype of *Dirofilaria*, initially found in humans in Hong Kong, was described using a combined morphological and molecular approach. The findings reveal that *D. asiatica* sp. nov. differs significantly from other known species, including *D. repens* and *D. immitis*, and might be responsible for the majority of zoonotic *Dirofilaria* infections in southern and southeastern Asia. Furthermore, the identification of cryptic *Dirofilaria* spp. in both canine and human hosts emphasises the importance of molecular tools for specific identification, particularly when morphological information is inadequate. This study provides insights into the taxonomy and zoonotic potential of *D. asiatica* sp. nov., as well as its relationship with related species of onchocercids. This combined morphological and molecular approach establishes a framework for future investigations of filarioid nematodes, with implications for improving diagnosis and understanding of their epidemiology in both veterinary and medical contexts.
© 2025 The Author(s). Published by Elsevier Ltd on behalf of Australian Society for Parasitology. This is an open access article under the CC BY license (http://creativecommons.org/licenses/by/4.0/).

1. Introduction

Parasitic nematodes of the family Onchocercidae (superfamily Filarioidea) have been associated with their vertebrate hosts since at least the Mesozoic (250 to 66 million years), with a major expansion occurring during the diversification of birds and mammals in the Cenozoic (Bain, 2002). Today, these nematodes remain major contributors to debilitating and potentially fatal diseases in a large range of hosts including humans, companion animals, and reptiles (Bain, 2002). Molecular phylogenetic investigations have classified nematodes of the family Onchocercidae into five distinct clades (ONC1 to ONC5) (Lefoulon et al., 2015). Members of ONC3, including *Onchocerca* and *Dirofilaria*, are of particular importance as pathogens of humans and animals (Lefoulon et al., 2015). For instance, infection with adult *Dirofilaria immitis* (Leidy, 1856) can cause life-threatening cardiopulmonary disease in dogs (McCall et al., 2008; Bowman and Atkins, 2009; Noack et al., 2021). However, the routine use of preventive chemotherapy with macrocyclic lactones has significantly reduced the prevalence of heartworm disease in dogs in high- and middle-income countries (Montoya-Alonso et al., 2010; Diakou and Prichard, 2021).

While the epidemiology, morbidity, and control measures of *D. immitis* are well-documented (Simon et al., 2012), there are still significant gaps in our knowledge of the diversity of species of many onchocercids and their impact on animal and human health (Simon et al., 2012; Otranto and Deplazes, 2019; Ramos et al., 2024). Traditionally, specific identification of parasites has been based on their morphological features and measurements. However, the specific identification is frequently not possible using morphology and morphometrics alone, because often there are very few characters that allow specific identification and

* Corresponding author.
E-mail address: vito.colella@unimelb.edu.au (V. Colella).

https://doi.org/10.1016/j.ijpara.2025.04.006
0020-7519/© 2025 The Author(s). Published by Elsevier Ltd on behalf of Australian Society for Parasitology.
This is an open access article under the CC BY license (http://creativecommons.org/licenses/by/4.0/).

differentiation, such that complementary molecular approaches need to be employed (Nadler and Perez Ponce de León, 2011; Lefoulon et al., 2015; Gasser et al., 2024). In addition, the varied locations of filarioid nematodes within host tissues can make collecting adult specimens and assigning them to species challenging (Lefoulon et al., 2015). Moreover, the long evolutionary history of filarioid nematodes with their host species has likely led to the speciation of onchocercid nematodes that are morphologically similar but genetically distinct (i.e. cryptic) species (Chabaud and Bain, 1994). The inability to accurately identify and distinguish species using morphology alone presents challenges for the specific diagnosis of infection and limits our ability to appreciate the clinical importance and epidemiology of onchocercid nematodes that have not yet been accurately described or discovered.

For instance, the zoonotic and clinical significance of select members of the genus *Dirofilaria* is still unclear or unknown (Simon et al., 2012; Otranto and Deplazes, 2019; Ramos et al., 2024). A particularly interesting example is a genotype of *Dirofilaria* that was first identified in three human patients in Hong Kong (To et al., 2012). Patients initially presented with cervical lymphadenopathy, an abdominal subcutaneous mass or a subconjunctival nodule, and by using a partial sequence of the cytochrome *c* oxidase subunit 1 gene (*cox*1; 321 bp, GenBank accession no. JX187591 and JX187599) and a nuclear ribosomal DNA region (ITS-1; 237 and 376 bp, accession no. JX290194 and JX290194, respectively), the same genotype of *Dirofilaria* was also identified in 3% of dogs (*Canis lupus familiaris*) studied in a nearby geographic location (To et al., 2012). The comparison of this genotype with the congeners *D. immitis* and *Dirofilaria repens* Railliet and Henry, 1911 revealed marked genetic differentiation (10.7% and 3.8% in the *cox*1, and 6.1% and 6% in the ribosomal region, respectively). In a subsequent study (Atapattu et al., 2023), subclinically infected dogs in Sri Lanka were identified as harbouring this novel genotype of *Dirofilaria* at a prevalence of up to 27.9%. Based on these findings, it is possible that dogs with subclinical infections could act as a reservoir for human infection(s). In humans, this novel *Dirofilaria* genotype has been associated with diverse clinical manifestations such as subcutaneous and subconjunctival nodules (Winkler et al., 2017; Xing et al., 2020; Kumar et al., 2021; Tirakunwichcha et al., 2022; Cope et al., 2024; Harch et al., 2024), which often require surgical removal and carry a risk of anaphylactic reactions (Luk et al., 2021). These nodules can be confused with benign or malignant tumours (Capelli et al., 2018; Schroeder et al., 2023) due to limited awareness among physicians and surgeons of the clinical relevance of dirofilariasis.

To et al. (2012) originally designated this genotypoed as "*Candidatus* Dirofilaria hongkongensis". However, under the International Code of Zoological Nomenclature (ICZN), the lack of a detailed morphological description of adult worms, as well as the lack of a designated holotype, renders "*Candidatus* D. hongkongensis" a nomen nudum (Dantas-Torres and Otranto, 2020). Similarly, the species name "*Dirofilaria hongkongensis*," as used by Schroeder et al. (2023) and Xing et al. (2020), also constitutes a *nomen nudum* due to the absence of an accurate taxonomic characterisation.

Furthermore, the lack of genetic data from a morphologically characterised adult worm isolated from the canine host has limited our ability to assess the zoonotic potential of this taxon. In this context, we undertook the first detailed morphological and molecular characterisation of *Dirofilaria* males, females, and microfilariae from dogs from Sri Lanka that were genetically consistent with the genotype originally studied by To et al. (2012) using *cox*1 and ITS-1 regions. We characterised the mitochondrial (mt) genome of this taxon and conducted a molecular phylogenetic analysis to compare it with related species of onchocercid nematodes. This combined morphological–molecular approach enabled us to describe *Dirofilaria asiatica* sp. nov. from the domestic dog *C. lupus familiaris*.

2. Materials and methods

2.1. Collection and morphological examination of adult specimens

Adult nematodes were collected from nodules within the testes, scrotum and/or spermatic cords from seven dogs during a neutering campaign in Puttalam (8°2′26.88″N, 79°50′21.84″E) as part of a nationwide survey on canine vector-borne pathogens in Sri Lanka – approved by the Committee for Ethical Clearance on Animal Research of the Faculty of Veterinary Medicine and Animal Science, University of Peradeniya, Sri Lanka (VERC/20/07). Following the nodule excision, adult nematodes were isolated and washed extensively in sterile physiological saline and fixed in 70% ethanol. Subsequently, specimens were cleared in lactophenol and examined using a light microscope Zeiss Axio Scope A.1 with differential interference contrast (DIC) optics. Specimens were drawn and measured using a Leitz drawing tube fitted to a Zeiss Ortholux microscope.

2.2. Collection of blood samples and molecular identification of microfilariae

Blood samples collected from the saphenous vein of domestic dogs in Puttalam, Sri Lanka, into ethylenediaminetetraacetic acid (EDTA) tubes were tested for filarioid nematodes using a modified Knott's test (MKT) (Atapattu et al., 2023) – with and without methylene blue (0.1%) staining. Slides were coverslipped and examined using a CX43 microscope (Olympus Life Sciences, Japan) at x400 and x1000 magnifications. For further study, only microfilariae from blood samples containing exclusively the *Dirofilaria* genotype reported previously by To et al. (2012) were used. An established nanopore-based metabarcoding method using the mt *cox*1 marker (Huggins et al., 2024) was employed to demonstrate that samples contained only this genotype.

2.3. Morphologic and morphometric study of microfilariae

Images of microfilariae were obtained using the CX43 microscope equipped with a DP23 digital camera (Olympus Life Sciences, Japan) and analysed using Olympus CellSense Entry 3.2 (Olympus corporation) software as well as using a DM1000 LED microscope (Leica, Germany) equipped with a Flexacam C3 camera (Leica) and analysed using LAS X Life Science Microscope Software (Leica). With both microscopes, the images for measurements were obtained using 200- and 400-times magnifications. The morphology and morphometry of microfilariae were evaluated using previously published keys (Orihel, 1961; Lindsey, 1965; Ananda et al., 2006; Demiaszkiewicz et al., 2011; Liotta et al., 2013; Potters et al., 2018; Magnis et al., 2013).

Measurements were taken using ImageJ 1.54 (Schneider et al., 2012). Data collected for each microfilaria were recorded in a Microsoft Excel spreadsheet, cleaned in RStudio (R. Core Team, 2022) using the packages 'tidyverse' and 'janitor'. To assess the effect(s) of methylene blue staining, the length measurements of the microfilariae were subjected to a two-way ANOVA, following a normality check via a normal Q-Q (Quantile-Quantile) plot. Descriptive statistics for microfilarial metrics were calculated using the cleaned dataset using the package 'DescTools': Tools for descriptive statistics, R 0.99.47.

2.4. Extraction and mitogenomic sequencing of DNA from a single adult worm

A single adult female worm extracted from a nodule from a dog from Puttalam (Sri Lanka) was washed in physiological saline and stored in ethanol 70%. High quality genomic DNA (~220 ng) was isolated from an anterior-body section (10–15 mm) of this worm using an established protocol (https://brindleylab.smhs.gwu.edu/extraction-genomic-dna-single-adult-schistosome; Brindley et al., 1989). An aliquot of genomic DNA (14 ng) was subjected to PCR-based *cox*1 sequence analysis (Casiraghi et al., 2001) to show that it was genetically consistent with the *Dirofilaria* genotype reported previously by To et al. (2012). Subsequently, genomic DNA (~220 ng) from this same worm was amplified using the REPLI-g midi kit (Qiagen, Germany) to produce 29 µg of DNA. The integrity of both the original and the amplified genomic DNA was verified using an Agilent 4200 TapeStation system (ThermoFisher, USA) and Genomic DNA ScreenTape (ThermoFisher, USA). A SMRTbell DNA library was constructed from 15 µg of the amplified DNA and then sequenced using the PacBio-HiFi Revio sequencing platform (PacBio, USA).

Long sequence reads obtained from the PacBio-HiFi Revio sequencer were mapped to individual reference mt genomes available for *Dirofilaria* spp. (NCBI accession nos. NC_031365.1, KX265049.1, KX265048.1, NC_029975.1, KX265047.1 and NC_005305.1) using Minimap2 v.2.0 (Li, 2018). These mapped reads were then assembled de novo using FLYE v.2.6 (Kolmogorov et al., 2019) employing the –pacbio-hifi option. The annotation of tRNA, rRNA and protein-encoding genes was initially undertaken using the MITOS v.2 (Bernt et al., 2013) employing the mt genetic code for invertebrates (https://www.ncbi.nlm.nih.gov/Taxonomy/Utils/wprintgc.cgi; translation table 5) and the MITOS RefSeq89o database. Genes (named as recommended by Le et al., 2000), and translation initiation and termination codons were manually curated based on comparisons with those reported previously for *D. immitis* (see Hu et al., 2003). The inferred amino acid sequences and codon usages of protein-coding genes were manually verified and curated using Geneious Prime v.2024.0.3 (Kearse et al., 2012) employing the invertebrate mt genetic code. The assembled mt genome was aligned with those published for "*Dirofilaria* sp. hongkongensis" (KX265050; Yilmaz et al., 2016), *D. repens* (KX265047; Yilmaz et al., 2016) or *D. immitis* (AJ537512; Hu et al., 2003) using clustal omega v.1.2.4 (Sievers and Higgins, 2018). Nucleotide diversity (π) across the entire alignment was inferred by sliding window analysis (300 bp; 10 bp steps) using the R package pegas v.1.3 (Paradis, 2010); this diversity was plotted against midpoint positions in each window, and gene boundaries were defined using the R package ggplot2 (Wickham, 2016).

2.5. Mitogenomic differences and phylogenetic analyses

The DNA sequences of the 12 mt protein-coding genes and encoded amino acid sequences were each trimmed using trimAl (Capella-Gutiérrez et al., 2009), aligned separately using MAFFT employing the 'linsi' iterative refinement method (Katoh et al., 2019) and concatenated using Geneious Prime v. 2024.0.7. The sequences were aligned with respective sequences representing several onchocercid genotypes (*Dirofilaria* sp. Hong Kong genotype, *Dirofilaria* sp. 'Thailand II', *D. immitis*, *D. repens*, *Onchocerca flexuosa*, *Onchocerca ochengi*, *Onchocerca volvulus*, *Brugia malayi*, *Brugia pahangi*, *Brugia timori*, *Loa loa*, and *Wuchereria bancrofti*) and with that of *Setaria digitata* (outgroup; accession no. GU138699). Nucleotide and amino acid sequence differences were calculated upon pairwise comparison using MEGA software. Phylogenetic analyses were conducted using the concatenated/aligned nucleic acid or amino acid sequences representing all 12 mt protein-coding genes employing the Bayesian inference (BI) algorithm in MrBayes v.3.2.7 (Ronquist et al., 2012). For DNA sequence data, the optimal partitioning schemes and substitution model for the BI analyses were determined using ModelTest-NG v.0.1.6 (Darriba et al., 2020), with a model selection set to the Akaike information criterion and greedy search algorithm (Supplementary Method S1). The BI analysis was conducted with four chains each of 2 million Markov chain Monte Carlo iterations, sampling every 200 generations for four independent runs. Convergence was determined by the average standard deviation of split frequencies of > 0.01, with the potential scale reduction factor approaching 1. The first 25% of the sampled trees were discarded as burn-in, and the Bayesian consensus tree was constructed from the remaining trees. The BI trees were displayed in FigTree v1.4.4 (https://tree.bio.ed.ac.uk/software/figtree/).

3. Results

3.1. Morphological description of Dirofilaria asiatica sp. nov.

As a basis for a comprehensive morphological investigation and a description of the species (see section 3.2), we used four single male and 12 female adult specimens of *Dirofilaria* (from seven dogs from Puttalam) that were shown to be identical in the *cox*1 sequence (accession nos. JX187591 and JX187599) to the *Dirofilaria* sp. Hong Kong genotype reported previously by To et al. (2012).

General. Slender whitish filarioid with very small apical mouth opening (2 µm in diameter), surrounded by eight cephalic papillae and two lateral amphids. Body diameter progressively tapering anteriad starting from the end of the oesophagus and then abruptly ending in an equally rounded and blunt anterior end. Cuticle with conspicuous longitudinal ridges (Fig. 1A). Ridges are longest over the lateral lines and become irregular in arrangement and shorter in length towards mid dorsal and mid ventral line (Fig. 1B). Ridges composed of small knobs, each above underlying fine transverse annulation (Fig. 1C). Single knobs protrude up to 13 µm above the epicuticle (Fig. 1C). The knobs measure 10.5 µm in diameter longitudinally and up to 14 µm transversely. Thick, multi layered cuticle.

Female. Measurements given represent the average of allotype and paratypes (n = 12), followed by the range in parentheses.

Body length: 121 mm (104–136 mm). Width at nerve ring: 304 µm (240–335 µm), at posterior end of oesophagus: 416 µm (370–500 µm), at vulva: 489 µm (370–560 µm), at midbody: 479 µm (400–620 µm) and at anus: 135 µm (80–170 µm).

Outer layer of cuticle at midbody 30 µm thick, inner layer of cuticle 57 µm thick followed underneath by comparatively thin muscular layer 24 µm thick, with cytoplasmatic processes forming an uneven inner surface towards the pseudocoelom. Muscular layer enlarged towards the anterior end, where large cytoplasmatic processes cushion uterine tubes and intestine (Fig. 2A, 2D, 3C). The four sectors of somatic muscles end abruptly as lobes around 90 µm from anterior end, 60 µm before posterior end, forming characteristic crown-shaped appearance (Fig. 2C, 3A).

Oesophagus 1059 µm long (915–1080 µm). Anterior end of oesophagus slightly enlarged (Fig. 2A, 3A), constriction at nerve ring at 306 µm (270–360 µm) from anterior end (Fig. 2A, 3A, 3B). Shortly posteriad to the nerve ring, oesophagus widens slightly to glandular part. Division inconspicuous. Intestine similar or smaller in diameter than posterior end of oesophagus (Fig. 2A). Vulva opening well behind oesophagus, at 2193 µm (1400–3900 µm) from anterior end. Vagina complex, 150 µm by 180 µm in cross section, and 250 µm long. Vagina consisting of small tube with two bends and a chamber. Microfilariae pass from uterus

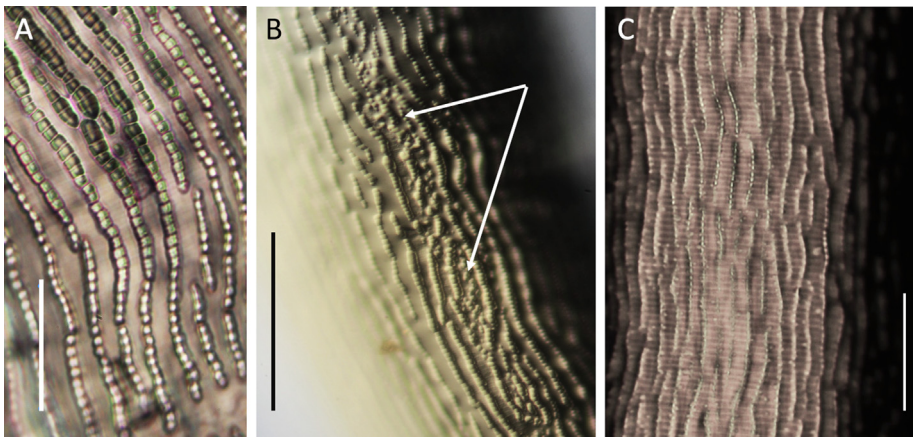


Fig. 1. Details of the cuticle of *Dirofilaria asiatica* sp. nov. female. Longitudinal ridges on sides (scalebar: 50 μm) (A). Note: Ridges formed by linearly arranged knobs. Ridges breaking up to single knobs in mid-ventral and mid-dorsal position (arrows; scalebar: 100 μm) (B). Longitudinal ridges and underlying transverse annulation (scalebar: 100 μm) (C).

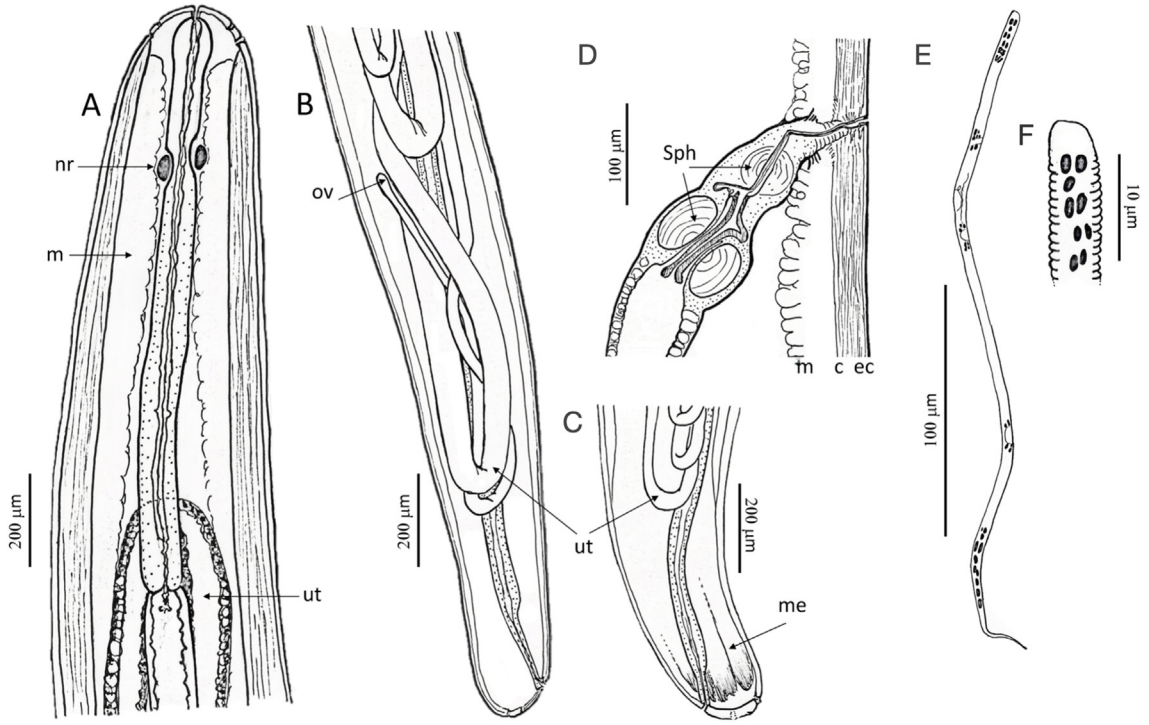


Fig. 2. Drawings of *Dirofilaria asiatica* sp. nov. female and microfilaria. Anterior end of female with isthmus of oesophagus at nerve ring (nr), thick body muscles (m), loop of uterus (ut) overlapping oesophagus (A); Posterior end with beginning of ovary (ov) and loops of small, young uterus (ut) (B); intestine (dotted) and anus. Posterior part of body bent dorsally with body muscles terminating in distinct line (me) (C). Longitudinal section of vulva and vagina with sphincter muscles (sph) (D), and details of structure of integument with longitudinal somatic muscles (m), fibrous cuticle (c), epicuticle separated by fine gap (ec) (D). Microfilaria appearance with distribution of head and tail nuclei (E). Anterior end nuclei and fine transverse annulation of the microfilaria (F).

through small tube into vagina, following narrow duct surrounded by large muscular sphincter. A narrow duct with additional sphincter with two bends that connect with vulva is present (Fig. 2D, 3C). In gravid females, the uterus is filled with numerous microfilariae (Fig. 3F). Ovaries close to posterior end. Loops of uterine tubes extending anteriad over oesophagus. In posterior part of body, ovarian tubes and uterine loops reach 500 μm (180–640 μm) from posterior end (Fig. 2A, 2B, 2C). Posterior body cavity filled with multiple parallel tubular regions of distal uterus (Fig. 3D), in anterior body, large uterine tubes appear compressed and entangled (Fig. 3E). Cells of uterine wall comparatively large, up to 35 μm in diameter (Fig. 2A, 2D). Body slightly tapers towards the caudal end, then abruptly terminates in a rounded extremity. Two phasmids are present close to the end of the tail. The terminal 600 μm portion of the tail ends curved dorsally in 11 out of 12 females, and straight in one sample (Fig. 2C bent dorsally, 2B straight). Anus positioned 50 μm (15–100 μm) from posterior end.

Male. Measurements given represent the average of holotype and paratypes (n = 4), followed by the range in parentheses.

Body length 63.6 mm (62–65 mm), width at midbody: 315 μm (280–355 μm), slowly tapering anteriad to abruptly end in a rounded anterior end as seen in females. Width at oesophagointestinal junction: 302 μm (280–315 μm), width at nerve ring: 232 μm (230–235 μm). Cuticle with longitudinal ridges on top of

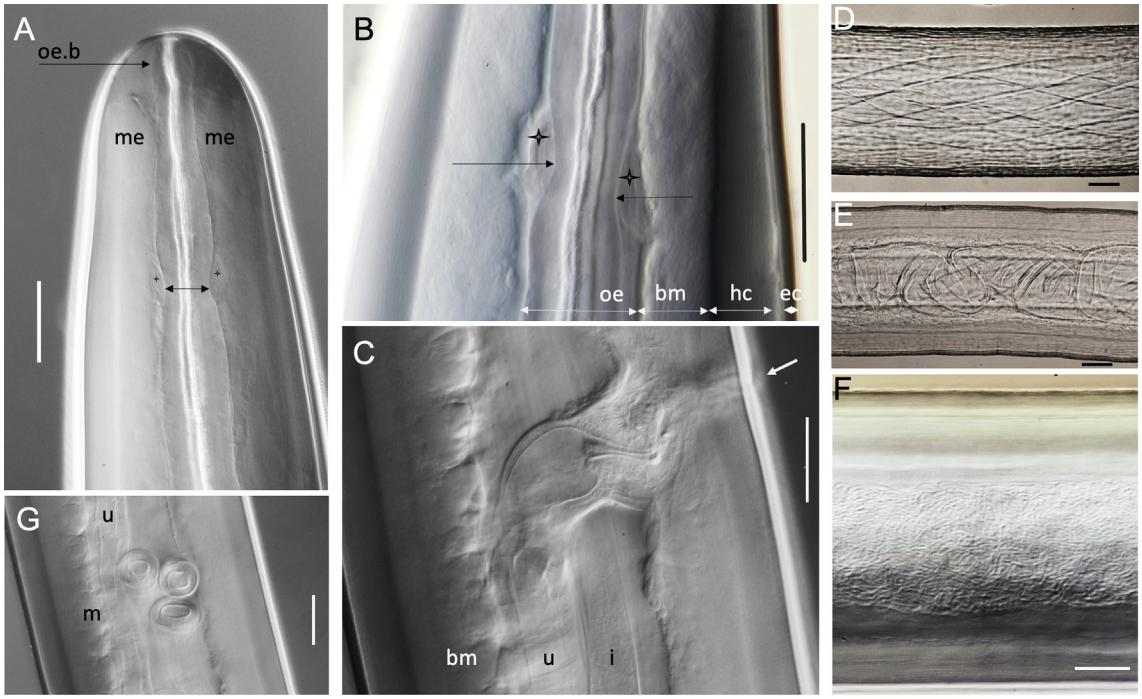


Fig. 3. Anterior end and genital tract of *Dirofilaria asiatica* sp. nov. female. Anterior end in longitudinal section showing swelling of anterior oesophagus (oe.b), ends of somatic muscles bands (me), isthmus of oesophagus (double arrow and nerve ring (crosses). Note: Somatic muscle cytoplasm contacting the oesophagus from both sides (A). Detail of oesophagus in longitudinal section with cross sections of nerve ring (stars), isthmus (arrows) of oesophagus. Oesophagus (oe); body muscles (bm); fibrous hypocuticle (hc); epicuticle (ec) (B). Complex structure of the vagina with two bends of vaginal duct (C). Vulva (arrow); somatic muscle cells with large enlarged cytoplasmatic processes (bm); uterus (u) with big cells; intestine (i) (C). Multiple ovarian tubes, appearing as plait, close to posterior end (D). Compressed part of uterus, midbody (E). Uterine tube filled with microfilariae, close to vagina (longitudinal section) (F). Three uterine loops in cross section, showing thick walls (longitudinal section) (G). Somatic muscles with cytoplasmatic processes (m); uterus in longitudinal section (u) (G). All scalebars: 100 µm.

fine transverse annulation. Circular constrictions may be seen towards posterior end (Fig. 4C). The ridges break up and disappear towards tail end, with only transverse annulation visible on subventral sides (Fig. 4D). The flattened ventral side is smooth (Fig. 4E). Cuticle consisting of two layers, separated by small gap, epicuticle and cuticle measuring 17 µm and 51 µm at midbody, respectively (Fig. 5A, 5C). Underlying longitudinal somatic muscle cells with large cytoplasm reaching out into pseudocoel. Inner lining of pseudocoel very uneven, measuring 57 µm at midbody (Fig. 5C). All four longitudinal sectors of somatic muscles end abruptly anteriorly (Fig. 5B).

Oesophagus length 797 µm (700–860 µm), oesophagus with isthmus at nerve ring present at 258 µm (250–265 µm) from anterior end (Fig. 5A), oesophagus posteriad to nerve ring changing inconspicuously to glandular part.

Posterior part of body forming two spirals. Tail length: 76 µm (60–95 µm) with small alae (Fig. 5D, 5E, 5F). Papillae distributed as shown in Fig. 5D and 4B, with slight variations in between specimens (Fig. 5E, 5F). Always five or six large, pedunculated precloacal papillae on left or right-side forming rows with last pedunculated papilla placed slightly post cloacal. One laterally elongated, unpaired papilla present anterior to the cloacal rim (Fig. 4B and 5E). Four additional papillae form transverse row midway to the tail tip. One or two additional small tail papillae can appear at the sides before or after the last row of 4 papillae. Two phasmids open laterally and close to tail tip. Spicules unequal in length and dissimilar. Left spicule 518 µm (490–590 µm) in length, with 320 µm long and narrow shaft and needle-like distal part of 270 µm in length and only 2 µm width (Fig. 5G). Right spicule 198 µm (180–220 µm) in length, tip broad and ventro-dorsally flattened, sides laterally rolled in ventrad, forming broad distal ventral groove (Fig. 5D, 5E, 5F, 5H).

3.1.1. Differential diagnosis of adults Dirofilaria asiatica sp. nov.

Dirofilaria asiatica sp. nov. exhibits longitudinal ridges and transverse annulations typical of nematodes within the subgenus *Nochtiella*. However, with the exception of *D. repens*, *D. asiatica* sp. nov. differs morphometrically and morphologically from other species in this subgenus. For example, while the male body length of *D. asiatica* sp. nov. (62–65 mm) overlaps with that of *Dirofilaria ursi* (51–93 mm), other characteristics, such as the length of the oesophagus in males (797 µm vs. 980 µm, respectively), the body length of the female (104–136 mm vs. 150–210 mm, respectively), and the posterior position of the vulva relative to the oesophagus in *D. asiatica* sp. nov., clearly differentiate it from *D. ursi* (Uni, 1983; Michalski et al., 2010). Similarly, although the body length of females of *Dirofilaria tenuis* (80–130 mm) falls within the range of that of *D. asiatica* sp. nov. (104–136 mm), other characteristics, such as the distance of the vulva from the anterior end (980–1600 µm vs. 1400–3900 µm, respectively) and the male body length (40–48 mm vs. 62–65 mm, respectively), distinguish the two species (McIntosh, 1954; Orihel and Beaver, 1965).

Morphological analyses in this study suggest that among the *Dirofilaria* species affecting dogs, *D. asiatica* sp. nov. shares the closest relationship with *D. repens*. Notably, while the body length of male *D. asiatica* sp. nov. falls within the range of *D. repens*, females of the former species are slightly shorter than those of the latter, with average measurements of 121 mm vs. 154 mm, respectively. In addition, females *D. asiatica* sp. nov. had a slightly longer oesophagus (1059 µm) and a vulva positioned farther from the anterior end (2193 µm) compared with *D. repens* (966 µm and 1555 µm, respectively). In males, *D. asiatica* sp. nov. has the nerve ring located farther from the anterior end (258 µm) and a longer oesophagus (797 µm) compared to *D. repens* (162 µm and 713 µm, respectively). A detailed comparison of the morphomet-

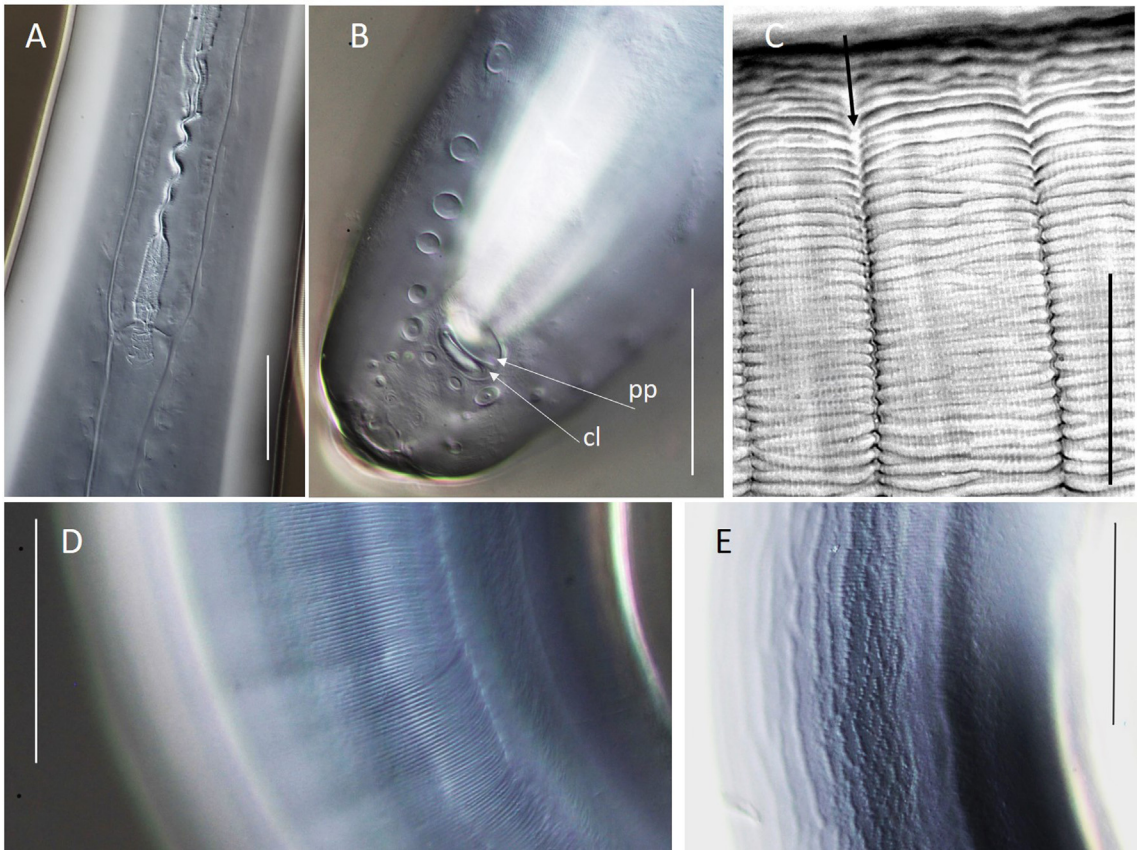


Fig. 4. *Dirofilaria asiatica* sp. nov. male. Cuticular lining of the oesophagus with variation in width and the oesophago-intestinal junction (A). Male tail, ventral view with distribution of papillae. Note: Precloacal unpaired papilla (pp), and cloaca (cl) with tip of right spicule appearing in it (B). Cuticular constrictions. Cuticle with longitudinal ridges and fine annulation. Transverse constrictions (arrow) appear in posterior part of body at irregular distances (C). Sublateral view of side of tail showing annulation and flattened and smooth concave side of tail (D). Tail region with ridges on dorsal side (E). All scalebars: 100 μm.

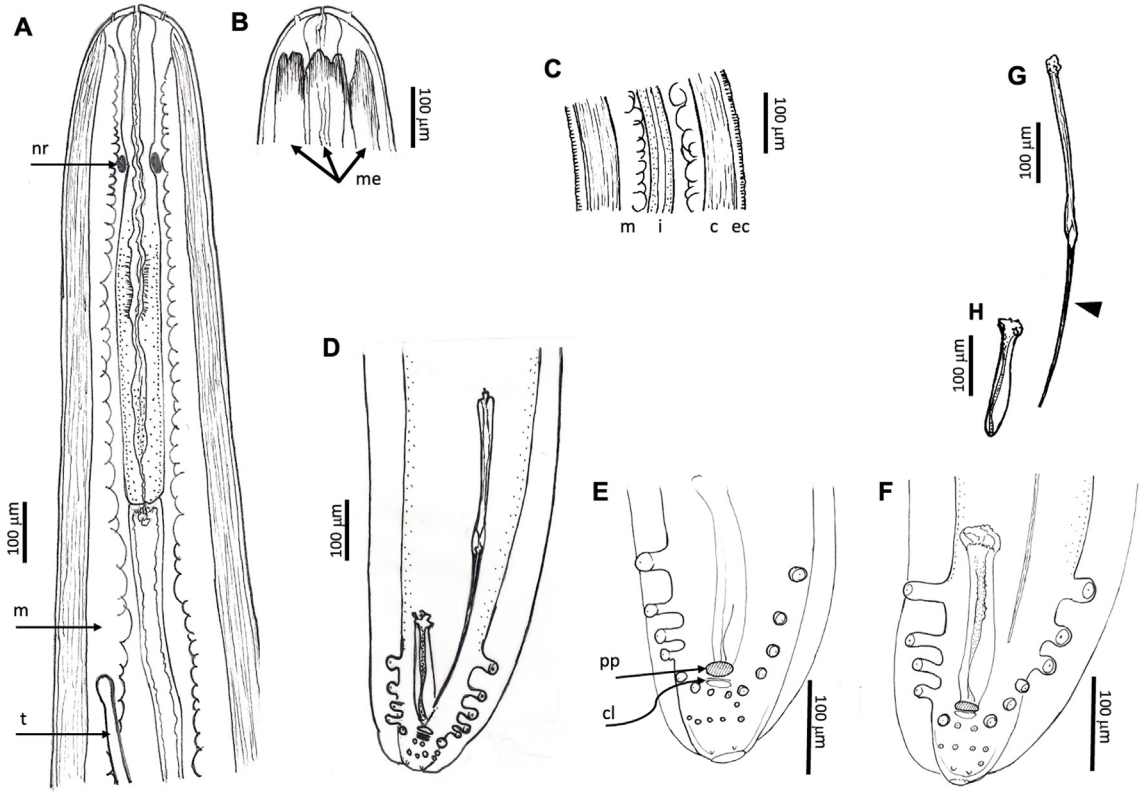


Fig. 5. Drawings of *Dirofilaria asiatica* sp. nov. male. Anterior end with nerve ring around isthmus of oesophagus (nr), thick layer of somatic muscles (m), testis (t) (A). Anterior end with somatic muscle bands (me) (B). Longitudinal section of body behind oesophagus; somatic muscles (m), intestine (i), cuticle (c); epicuticle with fine transverse annulation (ec) (C). Posterior end of male with distribution of papillae and alae (D). E and F some variation in arrangement and number of papillae in paratype specimens. Unpaired precloacal papilla (pp), cloacal opening (cl) (E). Left spicule with very fine distal process (arrowhead) (G). Right spicule, ventral view, with sides folded ventrad (H).

rics and morphological characteristics of adult male and female *D. asiatica* sp. nov. with those of *D. immitis* and *D. repens* from dogs is made in Table 1.

3.2. Taxonomic summary for adult specimens of Dirofilaria asiatica sp. nov.

Class **Nematoda Diesing, 1861**
Family **Onchocercidae Leiper, 1911**
Genus ***Dirofilaria*** **Railliet and Henry, 1911**
Subgenus ***Nochtiella*** **Faust, 1937**

Dirofilaria asiatica **sp. nov.**

Type-host: *Canis lupus familiaris* (Linnaeus, 1758) (Carnivora: Canidae).

Type-locality: Puttalam (8°2′26.88″N, 79°50′21.84″E), Sri Lanka.

Site in host: Spermatic cord.

Type-material: holotype (MHNG-INVE-0159628) and allotype (MHNG-INVE-0159629) deposited in the Muséum d'Histoire Naturelle in Geneva, Switzerland.

ZooBank registration: To comply with the regulations set out in article 8.5 of the amended 2012 version of the International Code of Zoological Nomenclature (ICZN, 2012), details of the new species have been submitted to ZooBank. The Life Science Identifier (LSID) for *Dirofilaria asiatica* sp. nov. is urn:lsid:zoobank.org:act:970FC69E-14D1-4ED9-BCD0-ED9C6C31A9B3.

Etymology: The species name refers to the geographic distribution of the parasite in Asia.

3.3. Morphological and morphometric description of D. asiatica sp. nov. microfilariae

For this part of the study, we used only samples shown to contain DNA from microfilariae that were genetically identical to *Dirofilaria asiatica* sp. nov. Following nanopore-based metabarcoding (see section 2.2), we showed that 41 blood samples of 41 dogs from Sri Lankan dogs contained *Dirofilaria asiatica* sp. nov. (16 other samples were inferred to contain multiple taxa; data not shown). Following sequence read filtering, the mean number of reads ± standard error (SE) for all 41 samples was 84,825 ± 5,286 (individual data sets are available from the NCBI database: BioProjectID PRJNA923029). This depth was considered as sufficient to accurately detect filarioid species present within individual samples (Huggins et al., 2024).

Table 1
Comparison of the morphometric and morphological characteristics of adult *Dirofilaria asiatica* sp. nov. with updated descriptions of adult *Dirofilaria immitis* and *Dirofilaria repens* collected from dogs. (Measurements show average, with range in parentheses).

		D. immitis	***D. repens***	***D. asiatica* sp. nov.**
Anatomical location in the definitive host		Right ventricle (heart), pulmonary arteries	Scrotum, subcutaneous connective tissues	Scrotum, subcutaneous connective tissues
Cuticular features (mid body) [a]		Transverse annulations	Conspicuous longitudinal ridges and fine transverse annulations	Conspicuous longitudinal ridges and fine transverse annulations
Male (number of specimens examined)		*n* = 7	*n* = 3	*n* = 4
Length (mm)		137.6 (119.4–162.3)	63 (56–70)	64 (62–65)
Distance to nerve ring from anterior end (μm)		400 (350–470)	162 (160–165)	258 (250–265)
Oesophagus length (μm)		1210 (1080–1460)	713 (696–730)	797 (700–860)
Posterior end		N/A	Well-developed cuticular alae spirally twisted in two turns	Small cuticular alae and spirally twisted in two turns
	Pre-cloacal papillae	1–6	5–6 on one side and 4–5 on the other	5–6 on one side always with variations between specimens
	Post-cloacal papillae	5 pairs	5	5–6
	Tail length	100 (90–110)	77 (73–82)	76 (60–95)
	Spicules			
	Left – length (μm)	340 (310–390)	541 (537–547)	518 (490–590)
	Left – shape	Stout shaft, distal part broader than shaft, tapering to tip	Long shaft with wide anterior part and thin distal part [b]	Long and narrow shaft, distal part very thin, needle-like
	Right – length (μm)	170 (150–190)	185 (181–189)	198 (180–220)
	Right – shape	N/A	Wide shaft with proximal end wider than distal part[b]	Distal part dorsoventrally flattened with rounded tip, sides laterally rolled inward ventrad, forming broad distal ventral groove
Female (number of specimens examined)		*n* = 18	*n* = 5	*n* = 12
Length (mm)		218.3 (177–272)	154 (147–161)	121 (104–136)
Distance to nerve ring from anterior end (μm)		410 (330–520)	295 (291–298)	306 (270–360)
Oesophagus length (μm)		1290 (1050–1570)	966 (915–1037)	1059 (915–1270)
Vulva	Distance from anterior end (μm)	2680 (2230–3260)	1555 (1445–1629)	2193 (1400–3900)
	Location	Posterior to the oesophageal-intestinal junction	N/A	Posterior to the oesophagus
References		Furtado et al. (2010)	Demiaszkiewicz et al. (2011)	The present study

[a] As shown in Wong and Brummer (1978) for *D. immitis* and *D. repens*.
[b] As shown in Yevstafieva et al. (2023).

Dirofilaria asiatica sp. nov. microfilariae (total number of 171) from 41 samples were examined and measured. Microfilariae examined microscopically were unsheathed (Fig. 6A) and possessed distinct features compared to *D. immitis*, such as a curved tail (Fig. 6B), the presence of cephalic space nuclei (Fig. 2E, 2F), cuticle with fine transverse annulations (Fig. 2F) and a rounded anterior end (Fig. 6C). They also presented a small subapical tooth. Nuclei distribution as shown in (Fig. 2E, 2F): Short cephalic space without nuclei, followed by 2-1-2-2-2 nuclei. Nerve ring present at 20.5%, excretory pore at 27.6%, excretory cell at 27.6% and last nuclei in tail at 89.7% of body length from anterior end. Nuclei-free tail end (10.3% of total body length) tapering to pointed tip. The morphological characteristics of the microfilariae found in canine blood are provided in Table 2.

A summary of the morphometric characteristics of *D. asiatica* sp. nov. microfilariae analysed in this study (n = 165) are presented in Table 3. Microfilariae of *Dirofilaria asiatica* sp. nov. had a mean total length of 300.3 μm when stained with 0.1% methylene blue and 312.8 μm when unstained. The mean width was 5.7 μm with 0.1% methylene blue and 5.9 μm without staining. A limited number (n = 6) of microfilariae were kept in 70% ethanol and showed a mean length and width of 293 μm and 5.9 μm, respectively.

Using a normal Q-Q plot, the length data of the microfilariae were confirmed to follow a normal distribution, and a two-way ANOVA was conducted. Microfilariae stained with methylene blue were significantly shorter than those that were unstained (P < 0.001).

A comparison of the morphometric characteristics of microfilariae species found in canine blood (i.e., *D. repens*, *D. immitis*, *Acanthocheilonema reconditum*, and *Acanthocheilonema dracunculoides*) with those of *D. asiatica* sp. nov. described in this study is provided in Table 4. The microfilariae of *D. asiatica* sp. nov. were substantially shorter than those of *D. repens* that can reach a mean length of 376 μm (Magnis et al., 2013). In addition, *D. asiatica* sp. nov. microfilariae were narrower than those of *D. repens* (Table 4).

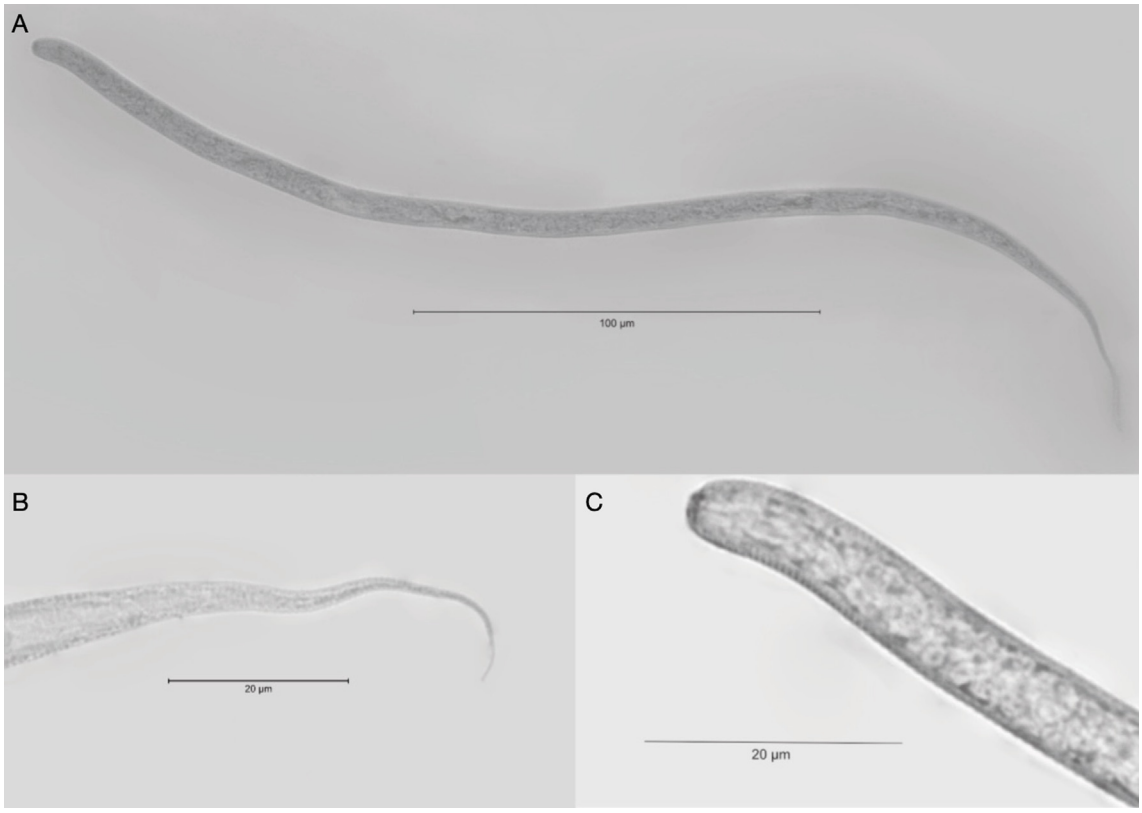


Fig. 6. Microphotographs of *Dirofilaria asiatica* sp. nov. microfilaria. Unsheathed microfilaria fixed in 2% formalin, observed at a 400 X magnification (A). Detailed features, including the curved tail (B) and rounded anterior end (C), were examined using oil immersion objectives (100 X magnification).

Table 2
Summary of morphological characteristics of species of *Dirofilaria* microfilariae found in canine blood.

Morphological characteristics	***Dirofilaria immitis***	***Dirofilaria repens***	***Dirofilaria asiatica* sp. nov.**
Sheath	Absent	Absent	Absent
Terminal tail shape	Straight	Curved	Curved
Nuclei in the tail tip	Absent	Absent	Absent
Cephalic space	Clear	2–3 nuclei	2–3 nuclei
Anterior head shape	Tapering	Round	Round
References	Lindsey (1965); Liotta et al. (2013)	Demiaszkiewicz et al. (2011); Liotta et al. (2013); Potters et al. (2018)	The present study

Table 3
Morphometric characteristics of *Dirofilaria asiatica* sp. nov. Microfilariae (*in* = 165) isolated from canine blood (*n* = 41), stained with 0.1% methylene blue.

	n	Mean (95% CI)
Total length (μm)	111	300.3 (297.2–303.5)
	54 [a]	312.8 (308.4–317.1)
Anterior end to final nucleus (μm)	43	268.43 (264.45–272.42)
Width (μm)	110	5.7 (5.6 – 5.9))
	54 [a]	5.9 (5.7 – 6.1)
Cephalic space length (μm)	17	3.27 (3–3.53)
Cephalic space width (μm)	44	4.43 (4.13–4.74)
Cephalic space Length:Width	17	0.64 (0.58–0.7)
Cephalic space Length:Total length (%)	14	1.06 (0.97–1.15)

n, no. of microfilariae; CI, confidence interval.
[a] Without 0.1% methylene blue.

3.4. Mitogenomic characterisation and comparison of *D. asiatica* sp. nov. with other onchocercid species/genotypes

The circular genome of *D. asiatica* sp. nov. (GenBank accession number PQ131197) is 13,647 bp in size (Fig. 7) and is used to complement the description of the species (see section 3.2). The key features of this mt genome, including the positions, lengths, and start/stop codons of individual genes as well as the amino acid sequence lengths of encoded proteins, are given in Supplementary Table S1. A + T and C + G contents of this genome are 76.3% and 23.7%, respectively. All 36 genes (22 *trn*, 12 protein-coding and 2 *rrn* genes) defined previously for members of the family Onchocercidae (onchocercids) (Hu et al., 2003) were identified; as expected, the *atp*8 gene is absent. All genes are transcribed in the same direction (Supplementary Table S1 and Fig. 8A).

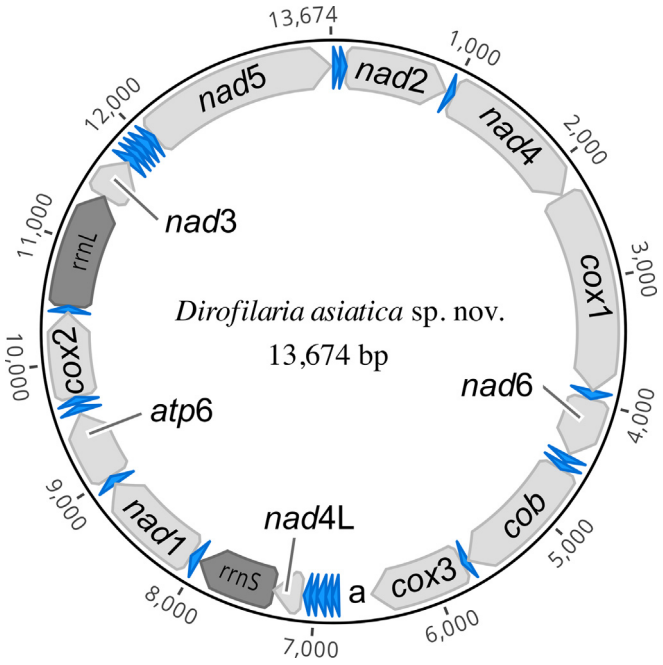


Fig. 7. Reference mitochondrial genome of *Dirofilaria asiatica* sp. nov. The circular mitochondrial genome from a single female adult worm was sequenced. Long (*rrn*L) and short (*rrn*S) rRNA subunits are shown in dark grey, protein-encoding genes are shown in light grey, while arrowheads represent transfer RNAs. The direction of gene transcription is indicated with an arrow. The position of the AT-rich control region is shown (a).

Table 4
Comparison of morphometric characteristics of species of microfilariae found in canine blood (i.e., *Dirofilaria repens*, *Dirofilaria immitis*, and *Acanthocheilonema dracunculoides* and *Acanthocheilonema reconditum*) with those of *Dirofilaria asiatica* sp. nov. described in the present study.

Species	Reference	Fixation method	Host	Location	Length (μm)		Width	
					Mean	S.D.	Mean	S.D.
A. dracunculoides	Muñoz at al. (2020)	MKT	Dog	Spain	260.8	6.85	5.88	0.55
A. reconditum	Cringoli et al. (2001)	MKT	Dog	Italy	265.2	10.1	5.01	0.49
A. reconditum	Magnis et al. (2013)	MKT	Dog	Italy	264.83	5.47	4.63	0.52
D. immitis	Magnis et al. (2013)	MKT	Dog	Greece, Italy, Portugal, Spain, Turkey	301.77	6.29	6.3	0.26
D. immitis	Cringoli et al. (2001)	MKT	Dog	Italy	311.3	9.5	5.96	0.15
D. immitis	Liotta et al. (2013)	Giemsa	Dog	USA	259.2	28.3	–	–
D. repens	Magnis et al. (2013)	MKT	Dog	Bulgaria, France, Greece, Italy, Romania, Spain, Hungary	369.44	10.76	8.87	0.58
D. repens	Demiaszkiewicz et al. (2011)	70% ethanol	Dog	Poland	329 (296–362)	–	7 (5–8)	–
D. repens	Cringoli et al. (2001)	MKT	Dog	Italy	366.2	12.1	6.4	0.31
D. repens	Potters et al. (2018)	MKT	Human	Belgium (source may be Senegal)	376 (357–395)	–	9.7 (7.5–10)	–
D. repens	Liotta et al. (2013)	Giemsa	Dog	Italy, Bulgaria, Poland, IDEXX EU	322.7	21.1	–	–
D. repens [a]	Mallawarachchi et al. (2018)	Giemsa	Dog	Sri Lanka	293	17.5	–	–
Dirofilaria sp. Hong Kong genotype (=*D. asiatica* sp. nov.)	Gowrishankar et al. (2019)	MKT and Giemsa	Dog	India	280–310	–	5–8	–
D. asiatica sp. nov.	The present study	MKT	Dog	Sri Lanka	With MB: 300.3 Without MB: 312.8	16.5 16	5.7 5.9	0. 7 0.7

MKT, Modified Knott's Test using 2% formalin; Giemsa, Giemsa-stained smears fixed in methanol, MB, 0.1% methylene blue.
[a] Potentially misidentified; likely *D. asiatica* sp. nov.

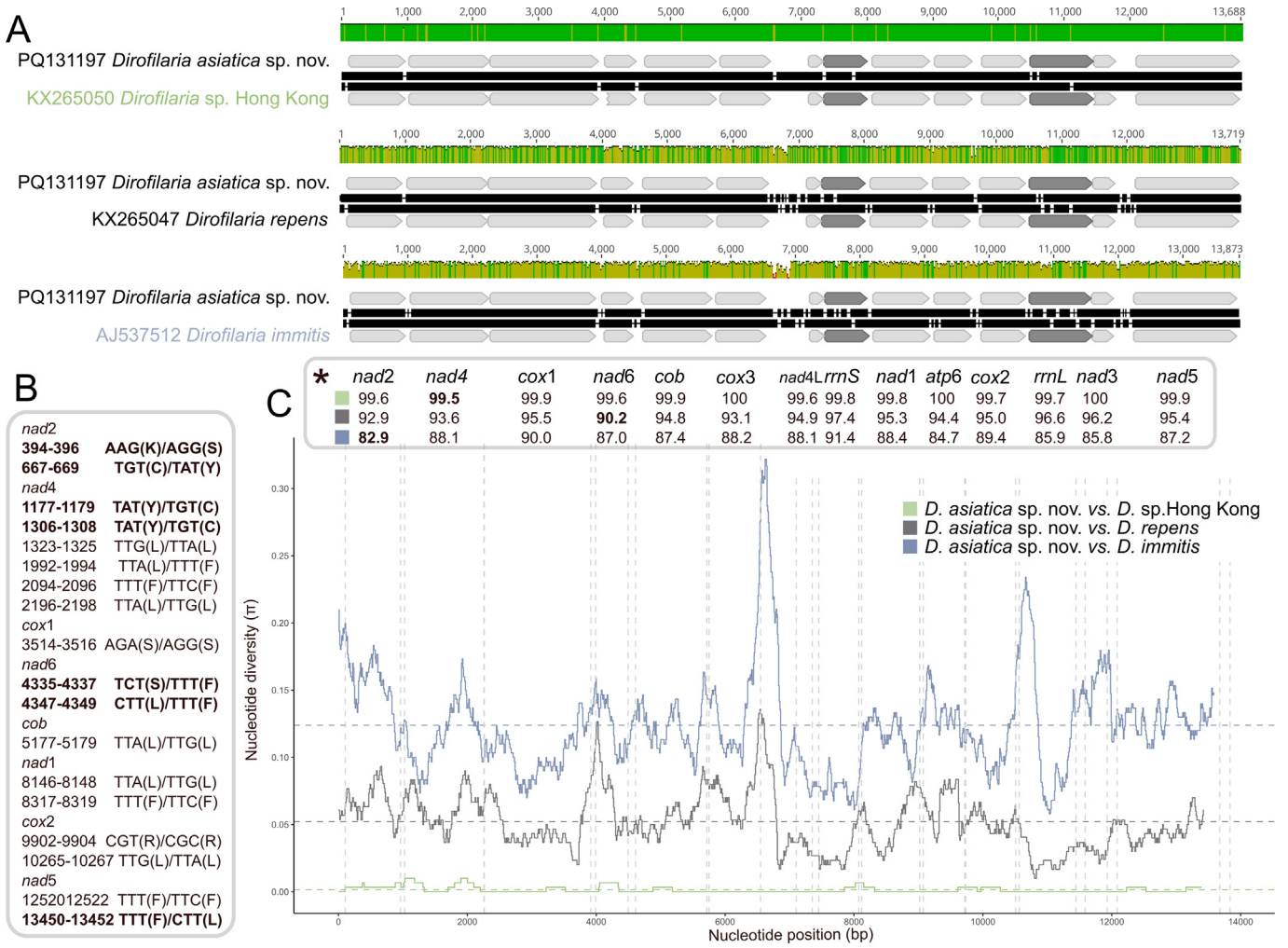


Fig. 8. Pairwise alignment of *Dirofilaria* mitochondrial genomes provides evidence of regional nucleotide diversity. The pairwise alignment of *Dirofilaria asiatica* sp. nov. with *Dirofilaria* sp. Hong Kong genotype, *Dirofilaria repens* or *Dirofilaria immitis* (A). The coloured bar plot above the aligned sequences (black solid lines) shows the percentage of identity between mitochondrial genomes with conserved regions shown in green, and less conserved regions shown in yellow or red. Protein-coding genes are shown in light grey and rRNA genes are shown in dark grey. Gaps are shown in the alignment by the spaces between the solid black lines. Nucleotide differences in codons between the mitochondrial genomes of *D. asiatica* sp. nov. and the *Dirofilaria* sp. Hong Kong genotype (B). Position within the alignment, codon and translated amino acid (NCBI translation table 5) are shown. Positions resulting in a non-synonymous nucleotide change are shown in bold (B). The nucleotide diversity (π) across each pairwise alignment (C). Nucleotide diversity was calculated in 300 bp sliding windows with a step size of 10 bp. Peaks in the plot indicate regions of high nucleotide diversity, suggesting genetic variation, while valleys indicate conserved regions. The average nucleotide identity within individual coding regions is shown (*); the lowest identity for each pairwise comparison is highlighted in bold (C).

Levels of nucleotide diversity between *D. asiatica* sp. nov. and other *Dirofilaria* species/genotypes were assessed via pairwise alignment and presence of localised nucleotide diversity (Fig. 8A). The mt genomes of *D. asiatica* sp. nov. and *Dirofilaria* sp. Hong Kong genotype had the highest pairwise identity (99.8%); in coding regions, 18 nucleotide differences between *D. asiatica* and *Dirofilaria* sp. "hongkongensis" were linked to codon alterations, seven of the 18 (38.9%) of which were non-synonymous single nucleotide polymorphisms (SNPs); most of this nucleotide variation (99.5%; 6 nucleotide differences) was linked to two non-synonymous SNPs) (Fig. 8B). The mt genomes of *D. asiatica* sp. nov. and *D. repens* had 94.2% nucleotide identity, with the *nad*6 gene being the most variable (9.8%) (Fig. 8C). The mt genomes of *D. asiatica* sp. nov. and *D. immitis* exhibited 86.1% nucleotide identity, with *nad*2 being most variable (17.1%) (Fig. 8C). Nucleotide diversity in the protein-coding regions between *D. asiatica* sp. nov. and other representative *Dirofilaria* species (upon pairwise comparison) revealed most diversity (mean: 0.124) with *D. immitis* (Fig. 8C) and least diversity (mean: 0.001) with *Dirofilaria* sp. "hongkongensis" (Fig. 8C). Most nucleotide diversity was detected in the genes *nad*2 and *cox*3 and least in *cox*1 and *nad*4L (Fig. 8C).

Extending the mitogenomic comparisons, we provided statistical support for the relationship of *D. asiatica* sp. nov. with other *Dirofilaria* spp./genotypes and related onchocercids through a phylogenetic analysis. At both the nucleotide and the amino acid levels (Fig. 9), *D. asiatica* sp. nov. clustered (pp: 1.0) with *Dirofilaria* sp. Hong Kong genotype (accession no. KX265050; Yilmaz et al., 2016) from a human from India. Together, these two taxa formed a monophyletic clade (pp: 1.0) with three specimens of *Dirofilaria* sp. 'Thailand II' from cats, positioning them as a sister group to *D. repens*, to the exclusion of *Dirofilaria immitis* from a dog from Australia. Three species of *Onchocerca* clustered together as a sister group to the exclusion of the well-supported clade of *Dirofilaria* spp. and genotypes (pp: 1.0). Species of *Brugia*, *Wuchereria* and *Loa* all grouped together (consistently pp: 1.0) (Fig. 9). The phylogenetic distance between *O. volvulus* and *O. ochengi* and among *B.*

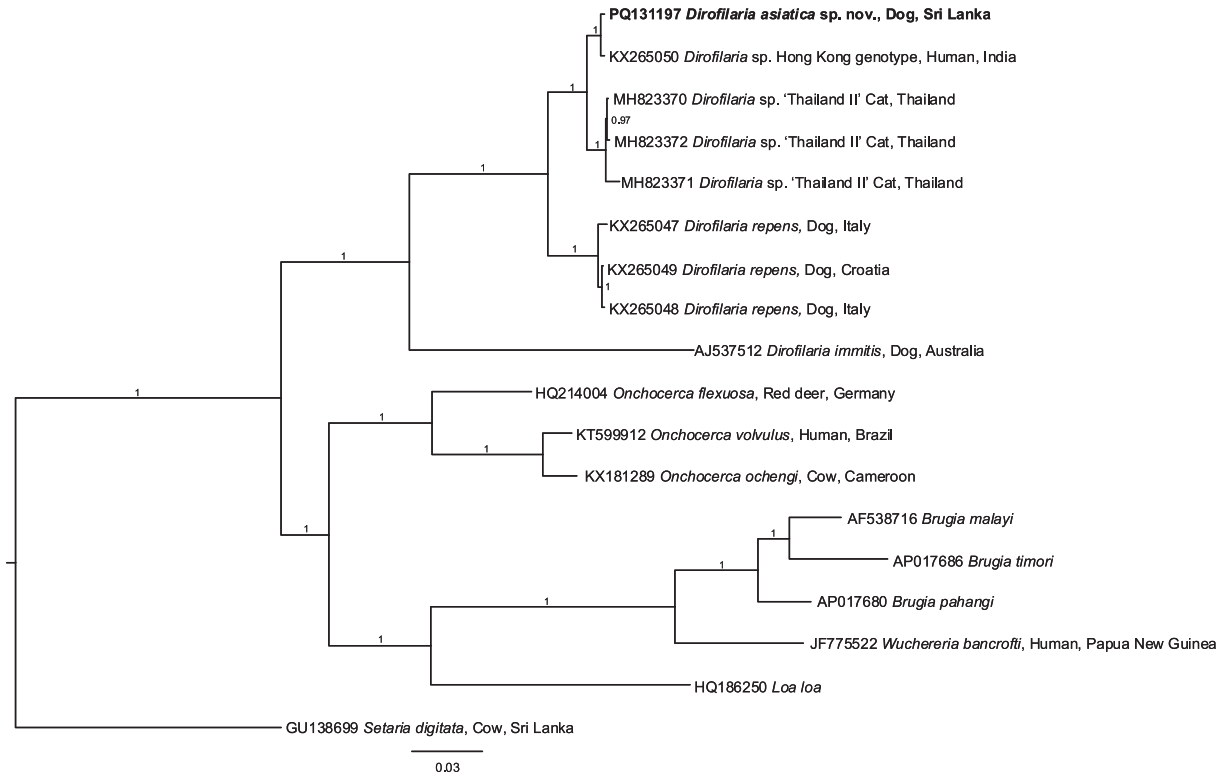


Fig. 9. Phylogenetic relationship of *Dirofilaria asiatica* sp. nov. with other representative filarioid nematodes. This phylogeny was inferred from concatenated nucleotide sequences derived from 12 mitochondrial protein-encoding genes using Bayesian inference (BI) analysis. Posterior probabilities of the BI analysis are indicated at each node of the tree. The scale bar indicates phylogenetic distance in substitutions per site. *Setaria digitata* is the outgroup.

malayi, *B. timori*, and *B. pahangi* are similar to that between *D. asiatica* and *D. repens*.

4. Discussion

Here, we provide a comprehensive morphological description of adult females, males, and microfilariae as well as a characterisation of the mt genome of a genotype of *Dirofilaria* from *C. lupus familiaris* that was genetically consistent to that described previously by To et al. (2012), to describe what we now call *D. asiatica* sp. nov.

Among the *Dirofilaria* spp. affecting dogs, the results of the present morphological analyses indicate that *D. asiatica* sp. nov. is most closely related to *D. repens*. With reference to the most recent redescription of the latter species (Demiaszkiewicz et al., 2011), *D. asiatica* sp. nov. females exhibit a slightly shorter body length, a longer oesophagus, and a vulva positioned further from the anterior end. In males, the oesophagus of *D. asiatica* sp. nov. is longer, and there are fewer pedunculated papillae on the tail, although this detail was not described in detail by Demiaszkiewicz et al. (2011). In addition, we conducted a comprehensive evaluation of the morphological and morphometric characteristics of *D. asiatica* sp. nov. microfilariae, and compared them with those of microfilariae from blood, for which published descriptions were available for *Dirofilaria* spp. (Orihel, 1961; Lindsey, 1965; Ananda et al., 2006; Demiaszkiewicz et al., 2011; Liotta et al., 2013; Magnis et al., 2013; Potters et al., 2018). This analysis is particularly relevant because microfilariae are typically the diagnostic stage for filarioids from canines, their recovery is simple and cost-effective, and species-level identification is important for an accurate diagnosis and appropriate treatment choice (Magnis et al., 2013). While no distinct morphological features were observed between the microfilariae of *D. asiatica* sp. nov. and *D. repens*, morphometric data, such as body length and width, were substantially different between these two species. Specifically, in a previous investigation (Magnis et al., 2013), *D. repens* microfilariae collected from several European countries (i.e., Bulgaria, France, Greece, Hungary, Italy, Romania, and Spain) were 369.4 μm long and 8.9 μm wide, whereas those of *D. asiatica* sp. nov., described herein, measured 300.3 μm and 5.7 μm, respectively. Conversely, microfilariae of *D. immitis* are similar in length and width to those of *D. asiatica* sp. nov., but are distinct in the presence of a curved rear end, the presence of cephalic space nuclei and a rounded anterior end (Orihel, 1961; Lindsey, 1965; Liotta et al., 2013). Further evaluations of *D. asiatica* sp. nov. collected from dogs across Asia will enable a thorough comparison and should help determine whether these features are consistent for this new species.

Dirofilaria asiatica sp. nov. and *D. repens* share many morphological and biological features, including the anatomical localisation of adult nematodes in animals and humans, and the presence of circulating microfilariae in dogs' blood. These similarities raise questions regarding the correct specific identification of the large number of earlier reports of *D. repens* in dogs and humans across southern and southeastern Asia, pre-dating the first report of this parasite (To et al., 2012), as hypothesised by Pradeep et al., (2019), and further complicate our understanding of the epidemiology of different species of *Dirofilaria*.

To tackle these obstacles, nucleic acid sequencing and complementary tools have enabled the specific identification and molecular systematic investigations of socioeconomically important species of parasitic nematodes (e.g., Nadler and Perez Ponce de León, 2011; Gasser et al., 2024). However, as conventional molecular techniques often only target one or a few pathogen species at a time, they may not identify co-infections and/or characterise novel pathogens. Recently, third-generation sequencing methods

such as nanopore-based long-read metabarcoding have proven effective in overcoming the limitations of traditional methods such as quantitative PCR (Huggins et al., 2024). For example, a novel long-read metabarcoding assay for filarial nematodes using the *cox*1 gene on the Oxford Nanopore Technologies' platform has enabled accurate identification and improved detection and characterisation of a diverse range of filarial worms from animals, humans, and arthropod vectors (Huggins et al., 2024). By using this novel platform, dogs in Sri Lanka were shown to be infected by *D. asiatica* sp. nov. only – with no evidence of the presence of *D. repens* – further strengthening the hypothesis that this novel species has been misidentified as *D. repens* (see Pradeep et al., 2019; Atapattu et al., 2023). This finding is particularly significant, given that Sri Lanka reports the highest number of subcutaneous dirofilariasis cases caused by *D. repens* globally, which is responsible for 54.5% of cases presenting with subcutaneous nodules in paediatric surgical departments (Wijekoon et al., 2022). The reliance on morphological features or single genetic markers for the specific identification of filarioids, combined with the discovery of only *D. asiatica* sp. nov. through a metabarcoding approach (cf. Huggins et al., 2024), suggests that many human cases previously attributed to *D. repens* might have been caused by *D. asiatica* sp. nov. However, the lack of comprehensive genetic data for isolates of *Dirofilaria* from dogs and humans hinders a sound understanding of the zoonotic potential of this species.

To address this knowledge gap, we defined here a reference mt genome of *D. asiatica* sp. nov. from a canine host. Phylogenetic analyses show that *D. asiatica* sp. nov., reported here, forms a strongly supported monophyletic clade with other specimens previously reported as the *Dirofilaria* sp. Hong Kong genotype from a human patient from India (Yilmaz et al., 2016). This finding provides further evidence for the role that dogs play as reservoirs of this zoonotic parasite (Atapattu et al., 2023).

The specific identification of *D. asiatica* sp. nov. is critical for foundational disciplines such as taxonomy and phylogeny, as well as for enhancing diagnosis and disease control. This holds importance because the use of single and/or conserved genetic markers for the molecular characterisation of parasites has the potential to lead to erroneous species attribution and may hinder our understanding of pathogen diversity and transmission. For instance, earlier suspicion of a novel zoonotic *Dirofilaria* spp. in Asia emerged from a report of a filarial infection in a German woman who, after travelling through India and Sri Lanka, presented with a subcutaneous nodule and meningoencephalitis (Poppert et al., 2009). This infection was attributed to *D. repens*, despite the 12S rDNA sequences (cf. Poppert et al., 2009) being 3% divergent from this species. In this case, the use of a conserved target gene was suboptimal. If less conserved gene targets had been utilised at the time, it is likely that sibling species might have been detected, potentially facilitating the identification of a novel species.

The present pairwise alignment of mt genomes of *Dirofilaria* (cf. Fig. 8) shows evidence of regional nucleotide diversity and provides detailed information on genetic variation in mt genes, providing a basis for the selection of target genes suited for distinguishing *D. asiatica* sp. nov., *D. repens* and *D. immitis*.

Clearly, the morphological description and the mt genome for *D. asiatica* sp. nov. provide a sound basis for future investigations of the systematics, population genetics, and epidemiology of members of the genus of *Dirofilaria* and related onchocercids. For instance, interspecific distances between well-defined species such as *O. volvulus* and *O. ochengi* were equivalent to those observed between *D. repens* and *D. asiatica* sp. nov., providing additional support for the status of the latter species. Genomic platforms are providing powerful tools for studies of enigmatic parasites and could be applied to other *Dirofilaria* of likely clinical and/or zoonotic importance, but of yet unknown specific status (cf. Simon et al., 2012; Ramos et al., 2024).

By combining molecular and morphological methods, the present approach has aided in delineating a taxon of zoonotic significance that might have been overlooked for decades. This combined approach becomes particularly relevant for filarial parasites, considering that their long-established parasitic nature has resulted in both the reduction of some morphological features and promoted convergent evolution, thus making morphology alone, less suited for phylogenetic analyses (Chabaud and Bain, 1994). Hence, the integration of molecular methods with traditional morphological and life history studies is expected to provide detailed phylogenetic information for this group of filarial nematodes (Lefoulon et al., 2015).

Interestingly, a high genetic variability among *Dirofilaria* isolates has been found across Asia, with many gene sequences linked to *D. asiatica* sp. nov. (cf. Yilmaz et al., 2016); this finding suggests that other as yet unknown cryptic species may occur within a species complex. To some extent, this is indicated by the formation of a strongly supported monophyletic clade with *Dirofilaria* sp. 'Thailand II' from cats. Since mt genomes might be maternally inherited in these nematodes, a well-curated nuclear genome for *D. asiatica* sp. nov. could pave the way for comprehensive population genetic analyses, offering insights into potential genetic exchange between different genotypes and aiding in elucidating the epidemiology of filarial parasites across the Asian continent.

CRediT authorship contribution statement

Vito Colella: Writing – review & editing, Writing – original draft, Supervision, Methodology, Investigation, Formal analysis, Conceptualization. **Neil D. Young:** Writing – review & editing, Visualization, Methodology, Investigation, Formal analysis. **Ralph Manzanell:** Writing – review & editing, Visualization, Methodology, Investigation, Formal analysis. **Ushani Atapattu:** Writing – review & editing, Visualization, Resources, Methodology, Investigation, Formal analysis, Data curation. **Sunita B. Sumanam:** Writing – review & editing, Methodology, Formal analysis. **Lucas G. Huggins:** Writing – review & editing, Methodology, Investigation, Formal analysis. **Anson V. Koehler:** Writing – review & editing, Visualization, Methodology, Investigation, Formal analysis. **Robin B. Gasser:** Writing – review & editing, Writing – original draft, Supervision, Methodology, Formal analysis, Data curation, Conceptualization.

Acknowledgements

The authors would like to thank Dr Chamari Medagoda, Dr Samith Ananda, Dr Menuka Karunasinghe, Mr Layan Mendis, and Ms Shalini Parakatawella for their assistance and logistical support in the field. The authors also thank Dr Aya Taki for her assistance with the imaging of microfilariae. The authors thank anonymous reviewers for their constructive reports on the manuscript. This study was funded partially by research funds to VC, and the Australian Research Council (LP180101334 – NYD and LP220200614 – RBG).

Appendix A. Supplementary material

Supplementary data to this article can be found online at https://doi.org/10.1016/j.ijpara.2025.04.006.

References

Ananda, K., D'Souza, P.E., Jagannath, M., 2006. Methods for identification of microfilaria of *Dirofilaria repens* and *Dipetalonema reconditum*. J. Vet. Parasitol. 20, 45–47.

Atapattu, U., Koehler, A.V., Huggins, L.G., Wiethoelter, A., Traub, R.J., Colella, V., 2023. Dogs are reservoir hosts of the zoonotic *Dirofilaria* sp. 'hongkongensis' and potentially of *Brugia* sp. Sri Lanka genotype in Sri Lanka. One Health 17, 100625.

Bain, O., 2002. Evolutionary relationships among filarial nematodes. Kluwer Academic Publishers, Boston, pp. 21–29.

Bernt, M., Donath, A., Jühling, F., Externbrink, F., Florentz, C., Fritzsch, G., Pütz, J., Middendorf, M., Stadler, P.F., 2013. MITOS: Improved de novo metazoan mitochondrial genome annotation. Mol. Phylogenet. Evol. 69, 313–319.

Bowman, D.D., Atkins, C.E., 2009. Heartworm biology, treatment, and control. Vet. Clin. North Am. Small Anim. Pract. 39, 1127–1158.

Capella-Gutiérrez, S., Silla-Martínez, J.M., Gabaldón, T., 2009. trimAl: a tool for automated alignment trimming in large-scale phylogenetic analyses. Bioinformatics 25, 1972–1973.

Brindley, P.J., Lewis, F.A., McCutchan, T.F., Bueding, E., Sher, A., 1989. A genomic change associated with the development of resistance to hycanthone in *Schistosoma mansoni*. Mol. Biochem. Parasitol. 36, 243–252.

Capelli, G., Genchi, C., Baneth, G., Bourdeau, P., Brianti, E., Cardoso, L., Danesi, P., Fuehrer, H.P., Giannelli, A., Ionica, A.M., Maia, C., Modry, D., Montarsi, F., Krucken, J., Papadopoulos, E., Petric, D., Pfeffer, M., Savic, S., Otranto, D., Poppert, S., Silaghi, C., 2018. Recent advances on *Dirofilaria repens* in dogs and humans in Europe. Parasit. Vectors. 11, 663.

Casiraghi, M., Anderson, T.J., Bandi, C., Bazzocchi, C., Genchi, C., 2001. A phylogenetic analysis of filarial nematodes: comparison with the phylogeny of *Wolbachia* endosymbionts. Parasitol. 122, 93–103.

Chabaud, A.G., Bain, O., 1994. The evolutionary expansion of the Spirurida. Int. J. Parasitol. 24, 1179–1201.

Cope, E.D., Gupta, N., Koehler, A.V., Gasser, R.B., Crowe, A., 2024. Ocular dirofilariasis in migrant from Sri Lanka, Australia. Emerg. Infect. Dis. 30, 829–830.

Darriba, D., Posada, D., Kozlov, A.M., Stamatakis, A., Morel, B., Flouri, T., 2020. ModelTest-NG: A new and scalable tool for the selection of DNA and protein evolutionary models. Mol. Biol. Evol. 37, 291–294.

Dantas-Torres, F., Otranto, D., 2020. On the validity of "Candidatus Dirofilaria hongkongensis" and on the use of the provisional status Candidatus in zoological nomenclature. Parasit Vectors 13 (1), 287.

Demiaszkiewicz, A.W., Polanczyk, G., Osinska, B., Pyziel, A.M., Kuligowska, I., Lachowicz, J., 2011. Morphometric characteristics of *Dirofilaria repens* Railliet et Henry, 1911 parasite of dogs in Poland. Wiad. Parazytol. 57, 253–256.

Diakou, A., Prichard, R.K., 2021. Concern for *Dirofilaria immitis* and macrocyclic lactone loss of efficacy: current situation in the USA and Europe, and future scenarios. Pathogens 10, 1323.

Gasser, R.B., Beveridge, I., Chilton, N.B., 2024. Molecular tools for systematic and epidemiological investigations of socioeconomically important parasitic nematodes of animals and humans. In: Tibayrenc, M. (Ed.), Genetics and Evolution of Infectious Diseases. Third Edition. Elsevier, Amsterdam, pp. 933–958.

Harch, S.A.J., Sheorey, H., Gasser, R.B., Cohen, P., Nelson, R., Koehler, A.V., 2024. Genital dirofilariasis involving the penile shaft, caused by *Dirofilaria* sp. Hong Kong genotype, Pathol (In Press).

Hu, M., Gasser, R.B., Abs El-Osta, Y.G., Chilton, N.B., 2003. Structure and organization of the mitochondrial genome of the canine heartworm, *Dirofilaria immitis*. Parasitol. 127, 37–51.

Huggins, L.G., Atapattu, U., Young, N.D., Traub, R.J., Colella, V., 2024. Development and validation of a long-read metabarcoding platform for the detection of filarial worm pathogens of animals and humans. BMC Microbiol. 24, 28.

ICZN, 2012. Amendment of Articles 8, 9, 10, 21 and 78 of the International Code of Zoological Nomenclature to expand and refine methods of publication. ZooKeys 219, 1–10.

Katoh, K., Rozewicki, J., Yamada, K.D., 2019. MAFFT online service: multiple sequence alignment, interactive sequence choice and visualization. Brief Bioinform. 20, 1160–1166.

Kearse, M., Moir, R., Wilson, A., Stones-Havas, S., Cheung, M., Sturrock, S., Buxton, S., Cooper, A., Markowitz, S., Duran, C., Thierer, T., Ashton, B., Meintjes, P., Drummond, A., 2012. Geneious Basic: An integrated and extendable desktop software platform for the organization and analysis of sequence data. Bioinformatics 28, 1647–1649.

Kolmogorov, M., Yuan, J., Lin, Y., Pevzner, P.A., 2019. Assembly of long, error-prone reads using repeat graphs. Nat. Biotechnol. 37, 540–546.

Kumar, A., Sreedhar, A., Biswas, L., Prabhat, S., Suresh, P., Asokan, A., Tomy, R.M., Vinod, V., Lakshmanan, B., Nambiar, A., Biswas, R., 2021. *Candidatus* Dirofilaria hongkongensis infections in humans during 2005 to 2020, in Kerala. India. Am. J. Trop. Med. Hyg. 104, 2046–2049.

Le, T.H., Blair, D., McManus, D.P., 2000. Mitochondrial genomes of human helminths and their use as markers in population genetics and phylogeny. Acta Trop. 77, 243–256.

Lefoulon, E., Bain, O., Bourret, J., Junker, K., Guerrero, R., Cañizales, I., Kuzmin, Y., Satoto, T.B.T., Cardenas-Callirgos, J.M., De Souza Lima, S., Raccurt, C., Mutafchiev, Y., Gavotte, L., Martin, C., 2015. Shaking the Tree: multi-locus sequence typing usurps current onchocercid (filarial nematode) phylogeny. PLOS Negl. Trop. Dis. 9, e0004233.

Lindsey, J.R., 1965. Identification of canine microfilariae. J. Am. Vet. Med. Assoc. 146, 1106–1114.

Liotta, J.L., Sandhu, G.K., Rishniw, M., Bowman, D.D., 2013. Differentiation of the microfilariae of *Dirofilaria immitis* and *Dirofilaria repens* in stained blood films. J. Parasitol. 99, 421–425.

Luk, B.W.C., Cheung, C.N., Chan, Y.F., 2021. Anaphylaxis after surgical excision of subcutaneous infection with parasitic *Dirofilaria*: a case report. Hong Kong Med. J. 27, 297–299.

Magnis, J., Lorentz, S., Guardone, L., Grimm, F., Magi, M., Naucke, T.J., Deplazes, P., 2013. Morphometric analyses of canine blood microfilariae isolated by the Knott's test enables *Dirofilaria immitis* and *D. repens* species-specific and *Acanthocheilonema* (syn. *Dipetalonema*) genus-specific diagnosis. Parasit Vectors. 6, 48.

McCall, J.W., Genchi, C., Kramer, L.H., Guerrero, J., Venco, L., 2008. Heartworm Disease in Animals and Humans. Elsevier, Amsterdam, pp. 193–285.

McIntosh, A., 1954. A new distribution record of *Dirofilaria tenuis* Chandler, 1942, and the discovery of the male. J. Parasitol. 40, 31–32.

Michalski, M.L., Bain, O., Fischer, K., Fischer, P.U., Kumar, S., Foster, J.M., 2010. Identification and phylogenetic analysis of *Dirofilaria ursi* (Nematoda: Filarioidea) from Wisconsin black bears (*Ursus americanus*) and its *Wolbachia* endosymbiont. J Parasitol. 96, 412–419.

Montoya-Alonso, J.A., Carretón, E., Juste, M.C., Mellado, I., Morchón, R., Simón, F., 2010. Epidemiological survey of canine heartworm disease on the island of Gran Canaria (Canary Islands – Spain) between 2000 and 2008. Vet. Parasitol. 173, 165–168.

Muñoz, C., Gonzálvez, M., Rojas, A., Martínez-Carrasco, C., Baneth, G., Berriatua, E., Ortiz, J., 2020. Massive microfilaremia in a dog subclinically infected with *Acanthocheilonema dracunculoides*. Parasitol Int. 76, 102070.

Nadler, S.A., Ponce, P., de León, G., 2011. Integrating molecular and morphological approaches for characterizing parasite cryptic species: implications for parasitology. Parasitol. 138, 1688–1709.

Noack, S., Harrington, J., Carithers, D.S., Kaminsky, R., Selzer, P.M., 2021. Heartworm disease – Overview, intervention, and industry perspective. Int. J. Parasitol. Drugs Drug Resist. 16, 65–89.

Orihel, T.C., 1961. Morphology of the larval stages of *Dirofilaria immitis* in the dog. J. Parasitol. 47, 251–262.

Orihel, T.C., Beaver, P.C., 1965. Morphology and relationship of Dirofilaria tenuis and Dirofilaria conjunctivae. Am. J. Trop. Med. Hyg. 14, 1030–1043.

Otranto, D., Deplazes, P., 2019. Zoonotic nematodes of wild carnivores. International Journal for Parasitology: Parasites and Wildlife 9, 370–383. https://doi.org/10.1016/j.ijppaw.2018.12.011.

Paradis, E., 2010. pegas: an R package for population genetics with an integrated–modular approach. Bioinformatics 26, 419–420.

Poppert, S., Hodapp, M., Krueger, A., Hegasy, G., Niesen, W.D., Kern, W.V., Tannich, E., 2009. *Dirofilaria repens* infection and concomitant meningoencephalitis. Emerg. Infect. Dis. 15, 1844–1846.

Potters, I., Vanfraechem, G., Bottieau, E., 2018. *Dirofilaria repens* nematode infection with microfilaremia in traveler returning to Belgium from Senegal. Emerg. Infect. Dis. 24, 1761–1763.

Pradeep, R.K., Nimisha, M., Pakideery, V., Johns, J., Chandy, G., Nair, S., Chandrasekhar, L., Ajithkumar, K.G., Deepa, C.K., Varghese, A., Ravindran, R., 2019. Whether *Dirofilaria repens* parasites from south India belong to zoonotic *Candidatus* Dirofilaria hongkongensis (*Dirofilaria* sp. hongkongensis)? Infect. Genet. Evol. 67, 121–125.

R. Core Team, 2022. R: A language and environment for statistical computing. Austria, Vienna.

Ramos, R.A.N., Hakimi, H., Salomon, J., Busselman, R.E., Curtis-Robles, R., Hodo, C.L., Hamer, S.A., Verocai, G.G., 2024. *Dirofilaria immitis* and *Dirofilaria striata* (Spirurida: Onchocercidae) detected in wild carnivores from Texas, United States. Int. J. Parasitol. Parasites Wildl. 24, 100954.

Ronquist, F., Teslenko, M., Van Der Mark, P., Ayres, D.L., Darling, A., Höhna, S., Larget, B., Liu, L., Suchard, M.A., Huelsenbeck, J.P., 2012. MrBayes 3.2: efficient Bayesian phylogenetic inference and model choice across a large model space. Syst. Biol. 61, 539–542.

Schneider, C.A., Rasband, W.S., Eliceiri, K.W., 2012. NIH Image to ImageJ: 25 years of image analysis. Nat. Methods. 9, 671–675.

Schroeder, J., Rothe, C., Hoerauf, A., Kroidl, I., Pfarr, K., Hübner, M.P., 2023. First case of *Dirofilaria hongkongensis* infection in Germany presenting as a breast tumour. J. Travel Med. 30, taad121.

Sievers, F., Higgins, D.G., 2018. Clustal Omega for making accurate alignments of many protein sequences. Prot. Sci. 27, 135–145.

Simon, F., Siles-Lucas, M., Morchon, R., Gonzalez-Miguel, J., Mellado, I., Carreton, E., Montoya-Alonso, J.A., 2012. Human and animal dirofilariasis: the emergence of a zoonotic mosaic. Clin. Microbiol. Rev. 25, 507–544.

Tirakunwichcha, S., Sansopha, L., Putaporntip, C., Jongwutiwes, S., 2022. Case report: An eyelid nodule caused by *Candidatus* Dirofilaria hongkongensis diagnosed by mitochondrial 12S rRNA sequence. Am. J. Trop. Med. Hyg. 106, 199–203.

To, K.K., Wong, S.S., Poon, R.W., Trendell-Smith, N.J., Ngan, A.H., Lam, J.W., Tang, T.H., AhChong, A.K., Kan, J.C., Chan, K.H., Yuen, K.Y., 2012. A novel *Dirofilaria* species causing human and canine infections in Hong Kong. J. Clin. Microbiol. 50, 3534–3541.

Uni, S., 1983. Filarial parasites from the black bear of Japan. Ann. Parasitol. Hum. Comp. 58, 71–84.
Wickham, H., 2016. ggplot2: Elegant graphics for data analysis. Springer-Verlag, New York.
Wijekoon, N., Antony, D., Muhunthan, T., Samarasinghe, M., 2022. Dirofilarial nodule as a differential diagnosis for subcutaneous lumps in children. Pediatric Surgery International 39 (1). https://doi.org/10.1007/s00383-022-05348-z.
Winkler, S., Pollreisz, A., Georgopoulos, M., Bago-Horvath, Z., Auer, H., To, K.K., Krucken, J., Poppert, S., Walochnik, J., 2017. *Candidatus* Dirofilaria hongkongensis as causative agent of human ocular filariosis after travel to India. Emerg. Infect. Dis. 23, 1428–1431.
Wong, M.M., Brummer, M.E.G., 1978. Cuticular morphology of five species of *Dirofilaria*: A scanning electron microscope study. J. Parasitol. 64, 108–114.
Xing, F., Li, X., Lo, S.K.F., Poon, R.W.S., Lau, S.K.P., Woo, P.C.Y., 2020. *Dirofilaria hongkongensis* infection presenting as recurrent shoulder mass. Parasitol. Int. 77, 102117.
Yevstafieva, V., Stybel, V., Melnychuk, V., Gutyj, B., Leno, M., Kravchenko, S., Kyrychko, O., Dmitrenko, N., Syzonenko, N., Opara, N., 2023. Description of the Nematode *Dirofilaria repens* (Nematoda, Onchocercidae) Parasitic in Dogs in Ukraine. Zoodiversity 57, 4.
Yilmaz, E., Fritzenwanker, M., Pantchev, N., Lendner, M., Wongkamchai, S., Otranto, D., Kroidl, I., Dennebaum, M., Le, T.H., Anh Le, T., Ramünke, S., Schaper, R., Von Samson-Himmelstjerna, G., Poppert, S., Krücken, J., 2016. The mitochondrial genomes of the zoonotic canine filarial parasites *Dirofilaria* (*Nochtiella*) *repens* and *Candidatus* Dirofilaria (Nochtiella) honkongensis provide evidence for presence of cryptic species. PLOS Negl. Trop. Dis. 10, e0005028.